

SUB-IMAGE RECAPTURE FOR MULTI-VIEW 3D RECONSTRUCTION

Yanwei Wang

Mixed Reality
Microsoft Corporation

ABSTRACT

3D reconstruction of high-resolution target remains a challenge task due to the large memory required from the large input image size. Recently developed learning based algorithms provide promising reconstruction performance than traditional ones, however, they generally require more memory than the traditional algorithms and facing scalability issue. In this paper, we developed a generic approach, sub-image recapture (SIR), to split large image into smaller sub-images and process them individually. As a result of this framework, the existing 3D reconstruction algorithms can be implemented based on sub-image recapture with significantly reduced memory and substantially improved scalability.

Index Terms— 3D reconstruction, multi-view geometry, photogrammetry, sub-image recapture

1. INTRODUCTION

3D object reconstruction from imagery has been an active research area for quite long time, with tremendous evolutions have been observed. Two main steps in a 3D reconstruction pipeline include a sparse modeling Structure-from-Motion (SfM) step and a dense modeling step Multi-View Stereo (MVS). The SfM undergoes a great deal of transformation and improvement over the years. Started from the early work [1, 2], increasingly large-scale reconstruction systems and variations have been developed [3]. Readers are referred to [4] for a survey and implementation of the current SfM algorithm. The MVS algorithm has also been advanced from early traditional MVS [5, 6, 7, 8] to neural net and learning based algorithms including both stereo [9, 10, 11, 12, 13, 14, 15] as well as MVS [16, 17, 18, 19, 20, 21, 22, 23, 24, 25, 26, 27] with improved accuracy and/or efficiency for various datasets. The learning based MVS algorithms hold the potential solution to hard problems such as variation of illumination, lack of texture or non-Lambertian surface, as well as occlusion [28].

However, these learning based MVS algorithms is known to have the scalability issue due to their high memory consumption. With today’s increasing camera sensor size as well

as the super-resolution techniques [29], the memory requirement increases geometrically. For example, a 10K by 10K resolution airborne image for 3D terrain reconstruction will use 1.2GB memory assuming floating point resolution for all RGB channels. For such scenario, even two-view stereo will has minimum memory requirement of 2.4GB, without considering the extra cost of any algorithm used. When the input image size is too large, down-sampling of the input image has to be performed to meet the memory requirement.

Considerable efforts have been observed in the literature to address this issue [26, 12, 21, 22, 23, 24]. All these works are trying to improve the performance from the algorithm point-of-view, with experimental maximum size *between a few hundreds to a couple of thousands* in width/height.

The framework introduced in this paper address this scalability issue from a data point-of-view, independent of the algorithms used. This solves the existing learning based MVS algorithm’s scalability problem once for all, the existed learning MVS algorithms can be applied to *any large image size* without down-sampling.

2. SIR: AN UNIVERSAL STRATEGY

We develop a sub-image recapture (SIR) approach which can be used to implement existing 3D reconstruction algorithms with reduced memory requirement and improved efficiency. In fact, it can be used for most 3D image processing algorithm which utilizes camera model.

The idea of sub-image recapture starts from splitting the original image into a matrix of smaller images which is referred to as sub-images. Unlike down-sampling, each sub-image has a smaller image size than the native image while maintaining the same native spatial resolution of the native image such that there is no loss of details. Each sub-image is then treated as an independent image which is “recaptured” by a corresponding synthesized camera with its own distinct camera parameters. Through this process, for each target pixel or area of interest, we have more “focused” sub-images instead of the original full field of view images to calculate the depth information.

The following advantages can be achieved by this approach: 1) significant memory reduction for each MVS step due to the use of sub-images; 2) under the fixed memory

limit, in multi-view geometry stage, more images could be used for the same target area hence the improved depth estimation accuracy; 3) for some applications where there are only partial overlaps between adjacent images, sub-image approach can enforce only overlapping part of the sub-images enter the MVS step hence has more efficient use of memory, 4) improved parallel implementation of the MVS algorithm due to the fact that the original image is split into sub-images which can be processed in parallel.

3. SYNTHESIZED RECAPTURE CAMERA

3.1. Definition of Recapture Camera

Recapture camera is best explained by dividing a native digital image into a matrix of sub-images. Each sub-image is associated with a distinct synthesized recapture camera which has synthesized intrinsic and extrinsic parameters mapped from a real camera associated with the native digital image. In particular, the synthesized intrinsic parameters for a sub-image's camera include a principal point which corresponds to the native digital image's principal point re-defined relative to the sub-image's coordinate system origin. Re-defining the native principal point relative to the sub-image's coordinate system origin spatially compensated all the location differences between the sub-image and its native parent, without any error involved. The lens distortion of the native image's camera will also be carried over to all its sub-images, and hence the undistortion process.

By associating each sub-image with a distinct synthesized recapture camera, each sub-image and associated synthesized recapture camera can be treated as a separate, full frame, digital image as if captured by a real camera in its entirety, only with a smaller field of view.

Figure 1(a) illustrates a camera model with 4×4 sub-images. As an example, the synthesized camera of sub-image index (2,1) is shown in Figure 1(a) and 1(b). Here $O(x_o, y_o)$ denotes the location of the sub-image (2,1)'s origin, $P(x_p, y_p)$ denotes the native principal point. The synthesized camera for sub-image (2,1) has its principal point defined as

$$P_{(2,1)}(x, y) = (x_p - x_o, y_p - y_o) \quad (1)$$

Note that the synthesized camera principal point could have a negative location value.

So for a native image size of $S_x \times S_y$ with a sub-image recapture configuration of $I \times J$, the principal points for each sub-image (i, j) is given by

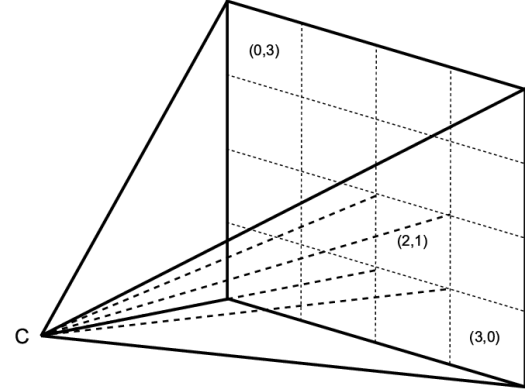
$$P_{(i,j)}(x, y) = (x_p - i \cdot \frac{S_x}{I}, y_p - j \cdot \frac{S_y}{J}) \quad (2)$$

where i and j denotes the index of sub-image at horizontal and vertical directions, respectively.

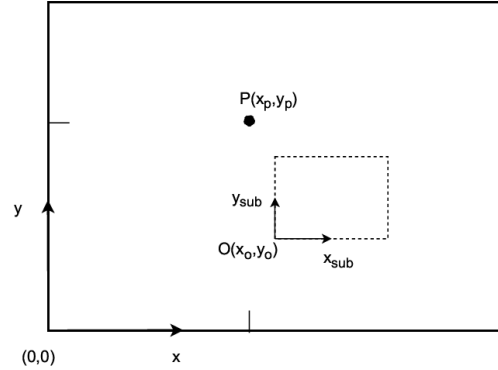
The elegance of sub-image recapture is, except for the principal point change, all other intrinsic and extrinsic camera parameters of the synthesized recapture camera associated

with each sub-image are kept the same as their corresponding native camera parameters.

Note that depending on application, sub-image recapture may be used to "recapture" an *arbitrary area and size* of the native image, not necessarily on a uniform grid of same sized sub-images.



(a) Camera with 4×4 sub-images



(b) principal point offset

Fig. 1. Cameras associated with both the original image and one of the corresponding 4×4 sub-images.

3.2. SIR for SfM and MVS

The SIR method can be applied to SfM step too. Generally speaking, higher resolution image will have better feature extraction and matching accuracy performance compared with its down sampled and blurred counterpart. However, if there are a lot of overlaps and less challenges between clustered images, the down sampled image may still work for SfM, thanks to the scale-invariant feature extraction and the powerful state-of-the-art SfM algorithms. Another observation from SfM is, it usually requires a single image each time during the feature extraction step, hence in terms of memory usage it is

not as demanding as MVS, which requires a group of images work together to infer the spatial information.

Since for the images we are experimenting with, the majority of the SIR improvements comes from MVS step, in this paper, we will focus on its performance on dense modeling.

3.3. SIR FOR 3D RECONSTRUCTION

Here we present a typical complete 3D pipeline for high-resolution reconstruction with sub-image recapture.

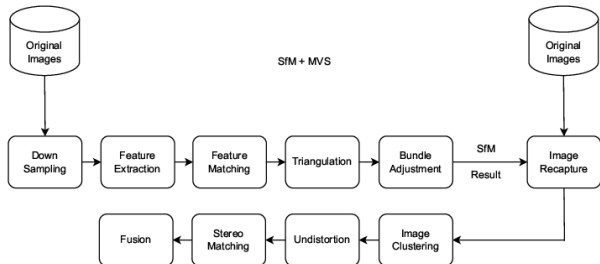


Fig. 2. 3D reconstruction pipeline.

Figure 2 shows the reconstruction pipeline used in the experiment with SfM followed by MVS step. Due to the large image size, the input to the SfM is decimated to a maximum size of 2304 to render a manageable image size for SfM. For the reason discussed in Section 3.2, we did not apply sub-image recapture for SfM in this dataset.

Some details of the pipeline: an incremental mapping [4] is used in SfM; an image clustering [30] step is used to group the overlapping sub-images for MVS; the recently proposed PatchmatchNet [28] has been used as the Stereo Matching step. For more details of each block in the pipeline, please refer to COLMAP [4], PatchmatchNet, and their related references.

4. EXPERIMENTS

4.1. Datasets

The data we used here is from a high altitude airborne terrain data provided by Vexcel Imaging, which covers the area of Angel Island, CA. The camera rig contains 5 cameras facing forward, backward, left, right, and nadir. The sizes of these native images are 10300×7700 , 7700×10300 , and 13470×8670 , with an average resolution of 7cm.

4.2. Implementation Details

Our implementation is based on the well-established open-source 3D reconstruction software COLMAP. A fork of

COLMAP has been developed to implement sub-image recapture. PatchmatchNet software is used as the stereo matching step.

The Angel Island has been divided into small tiles according to the Bing map tile system. Each tile at Level of Detail (LOD) 19 is processed with an NVIDIA GeForce RTX 2080ti with 11GB memory. At LOD 19, each tile has a size of approximately 40×40 meters.

A group of down-samplings between $5 \times$ to $6 \times$ are applied to the input images of SfM. The image clustering step is configured to generate a cluster size around 20.

The sub-image recapture is configured to have 5×5 sub-images for each native image. This configuration is chosen to have 2.3K maximum image size, which is about the upper limit our current MVS pipeline can handle. To compare the MVS result of SIR vs. without SIR (decimation), a down-sampling (resize) step is used to make sure that the MVS input image size has a maximum of 2304 pixels.

4.3. Experimental Results

Figure 3(a) and (b) show the comparison of a highly zoomed-in area of a target tile: decimated image with a close to a $5 \times$ stride vs. SIR with native resolution. Clearly, the decimated image shows blurred target features.

Figure 3(c) and (d) compare the reconstruction result point cloud between without SIR and with SIR, respectively, for a tile. SIR demonstrates much better reconstruction results due to the high-resolution sub-images it utilized.

Figure 4(a) and (b) show the Poisson surface reconstructed meshes from the result point cloud, without SIR and with SIR, respectively, by combining the output from multiple reconstructed tiles. The area shown is located at the east side of the island with buildings, vehicles, and trees. SIR’s mesh shows much clean result with better accuracy and resolution.

5. CONCLUSIONS

A Sub-Image Recapture (SIR) framework has been proposed and applied to high level-of-detail 3D reconstruction applications. Compared with the conventional down-sampling of the input image, SIR significantly outperforms its counterpart by retaining the native image’s resolution without degrading the image quality. To the best of our knowledge, this is the first time that state-of-the-art learning based MVS algorithm has been applied to the large images (13470×8670) used in the paper. Fundamentally, SIR solved the current memory-limited scalability problem and enabled the MVS algorithms to be applied to “*arbitrarily large*” images. It also provided improved accuracy and implementation efficiency. Based on COLMAP and PatchmatchNet, SIR is implemented as an open-source software and released to the public.



(a) Down-sampling



(b) Native



(c) without SIR

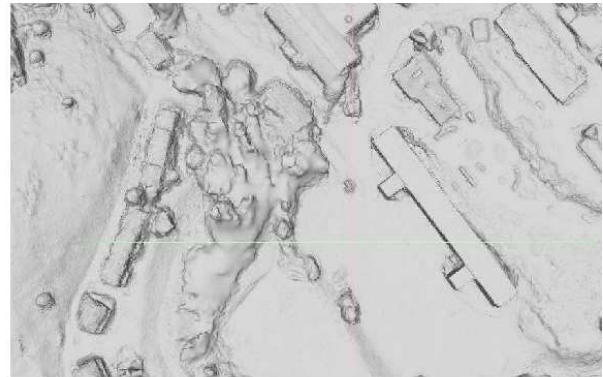


(d) with SIR

Fig. 3. A tile of the 3D terrain reconstruction point cloud.



(a) Down-sampling



(b) Sub-Image Recapture

Fig. 4. Mesh of a small area of the reconstructed 3D terrain.

6. REFERENCES

- [1] Paul Beardsley, Phil Torr, and Andrew Zisserman, “3d model acquisition from extended image sequences,” in *Computer Vision — ECCV ’96*, Bernard Buxton and Roberto Cipolla, Eds., Berlin, Heidelberg, 1996, pp. 683–695, Springer Berlin Heidelberg.
- [2] R. Mohr, F. Veillon, and L. Quan, “Relative 3-d reconstruction using multiple uncalibrated images,” in *Proceedings of IEEE Conference on Computer Vision and Pattern Recognition*, 1993, pp. 543–548.
- [3] Jared Heinly, Johannes L. Schönberger, Enrique Dunn, and Jan-Michael Frahm, “Reconstructing the world in six days,” in *2015 IEEE Conference on Computer Vision and Pattern Recognition (CVPR)*, 2015, pp. 3287–3295.
- [4] Johannes L. Schönberger and Jan-Michael Frahm, “Structure-from-motion revisited,” in *Proceedings of the IEEE Conference on Computer Vision and Pattern Recognition (CVPR)*, June 2016.

- [5] Sudipta Sinha, Philippos Mordohai, and Marc Pollefeys, “Multi-view stereo via graph cuts on the dual of an adaptive tetrahedral mesh,” in *International Conference on Computer Vision (ICCV)*, October 2007.
- [6] Yasutaka Furukawa and Jean Ponce, “Accurate, dense, and robust multiview stereopsis,” *IEEE Transactions on Pattern Analysis and Machine Intelligence*, vol. 32, no. 8, pp. 1362–1376, 2010.
- [7] Michael Bleyer, Christoph Rhemann, and Carsten Rother, “Patchmatch stereo - stereo matching with slanted support windows,” in *BMVC*, January 2011.
- [8] Silvano Galliani, Katrin Lasinger, and Konrad Schindler, “Massively parallel multiview stereopsis by surface normal diffusion,” in *2015 IEEE International Conference on Computer Vision (ICCV)*, 2015, pp. 873–881.
- [9] Yasutaka Furukawa, Brian Curless, Steven M. Seitz, and Richard Szeliski, “Towards internet-scale multi-view stereo,” in *CVPR*. 2010, pp. 1434–1441, IEEE Computer Society.
- [10] Yikang Ding, Zhenyang Li, Dihe Huang, Zhiheng Li, and Kai Zhang, “Enhancing multi-view stereo with contrastive matching and weighted focal loss,” in *2022 IEEE International Conference on Image Processing (ICIP)*, 2022, pp. 821–825.
- [11] Somi Jeong, Seungryong Kim, Bumsub Ham, and Kwanghoon Sohn, “Convolutional cost aggregation for robust stereo matching,” in *2017 IEEE International Conference on Image Processing (ICIP)*, 2017, pp. 2523–2527.
- [12] Alex Kendall, Hayk Martirosyan, Saumitro Dasgupta, Peter Henry, Ryan Kennedy, Abraham Bachrach, and Adam Bry, “End-to-end learning of geometry and context for deep stereo regression,” 2017.
- [13] Jia-Ren Chang and Yong-Sheng Chen, “Pyramid stereo matching network,” 2018.
- [14] Haofei Xu and Juyong Zhang, “Aanet: Adaptive aggregation network for efficient stereo matching,” 2020.
- [15] Jifeng Dai, Haozhi Qi, Yuwen Xiong, Yi Li, Guodong Zhang, Han Hu, and Yichen Wei, “Deformable convolutional networks,” 2017.
- [16] Mengqi Ji, Juergen Gall, Haitian Zheng, Yebin Liu, and Lu Fang, “SurfaceNet: An end-to-end 3d neural network for multiview stereopsis,” in *2017 IEEE International Conference on Computer Vision (ICCV)*. oct 2017, IEEE.
- [17] Abhishek Kar, Christian Häne, and Jitendra Malik, “Learning a multi-view stereo machine,” 2017.
- [18] Jingliang Li, Zhengda Lu, Yiqun Wang, Ying Wang, and Jun Xiao, “Ds-mvsnet: Unsupervised multi-view stereo via depth synthesis,” 2022.
- [19] Rui Chen, Songfang Han, Jing Xu, and Hao Su, “Point-based multi-view stereo network,” 2019.
- [20] Keyang Luo, Tao Guan, Lili Ju, Haipeng Huang, and Yawei Luo, “P-mvsnet: Learning patch-wise matching confidence aggregation for multi-view stereo,” in *2019 IEEE/CVF International Conference on Computer Vision (ICCV)*, 2019, pp. 10451–10460.
- [21] Yao Yao, Zixin Luo, Shiwei Li, Tian Fang, and Long Quan, “Mvsnet: Depth inference for unstructured multi-view stereo,” 2018.
- [22] Yao Yao, Zixin Luo, Shiwei Li, Tianwei Shen, Tian Fang, and Long Quan, “Recurrent mvsnet for high-resolution multi-view stereo depth inference,” 2019.
- [23] Xiaodong Gu, Zhiwen Fan, Zuozhuo Dai, Siyu Zhu, Feitong Tan, and Ping Tan, “Cascade cost volume for high-resolution multi-view stereo and stereo matching,” 2019.
- [24] Jiayu Yang, Wei Mao, Jose M. Alvarez, and Miaomiao Liu, “Cost volume pyramid based depth inference for multi-view stereo,” 2019.
- [25] Qingshan Xu and Wenbing Tao, “Pvsnet: Pixelwise visibility-aware multi-view stereo network,” 2020.
- [26] Zehao Yu and Shenghua Gao, “Fast-mvsnet: Sparse-to-dense multi-view stereo with learned propagation and gauss-newton refinement,” 2020.
- [27] Tak-Wai Hui, Chen Change Loy, and Xiaoou Tang, “Depth map super-resolution by deep multi-scale guidance,” in *Proceedings of European Conference on Computer Vision (ECCV)*, 2016.
- [28] Fangjinhua Wang, Silvano Galliani, Christoph Vogel, Pablo Speciale, and Marc Pollefeys, “Patchmatchnet: Learned multi-view patchmatch stereo,” 2020.
- [29] Thang Vu, Cao V. Nguyen, Trung X. Pham, Tung M. Luu, and Chang D. Yoo, “Fast and efficient image quality enhancement via desubpixel convolutional neural networks,” in *Computer Vision – ECCV 2018 Workshops*, Laura Leal-Taixé and Stefan Roth, Eds., Cham, 2019, pp. 243–259, Springer International Publishing.
- [30] Ondrej Chum and Jiří Matas, “Large-scale discovery of spatially related images,” *IEEE Transactions on Pattern Analysis and Machine Intelligence*, vol. 32, no. 2, pp. 371–377, 2010.